First publ. in: Fungal Genetics and Biology 43 (2006), pp. 8-19

Microarray analysis of expressed sequence tags from haustoria of the rust fungus *Uromyces fabae*

Mirza Jakupović [a], Manuel Heintz [a], Peter Reichmann [b], Kurt Mendgen [c], Matthias Hahn [a,*]

[a] *Department of Biology, University of Kaiserslautern, Post Box 3049, 67653 Kaiserslautern, Germany*
[b] *Center for Nanostructure Technology and Molecular Biological Technology, University of Kaiserslautern, Post Box 3049, 67653 Kaiserslautern, Germany*
[c] *Department of Biology, University of Konstanz, 78457 Konstanz, Germany*

Received 31 May 2005; accepted 9 September 2005
Available online 11 November 2005

Abstract

Rust fungi are plant parasites which colonise host tissue with an intercellular mycelium that forms haustoria within living plant cells. To identify genes expressed during biotrophic growth, EST sequencing was performed with a haustorium-specific cDNA library from *Uromyces fabae*. One thousand seventeen ESTs were generated, which assembled into 530 contigs. Several of the most frequently represented sequences in the EST database were identical to the in planta induced genes (*PIG*s) identified previously (Hahn, M., Mendgen, K., 1997. Characterisation of in planta-induced rust genes isolated from a haustorium-specific cDNA library, Mol. Plant–Microbe Interact. 10, 427–437). Virus-encoded sequences were identified, providing evidence for two novel RNA mycoviruses in *U. fabae*. Microarray hybridisation revealed many cDNAs that were significantly activated in rust-infected leaves compared to germinated uredospores. Very strong in planta expression was found for two *PIG*s encoding putative metallothioneins. Furthermore, several genes involved in ribosome biogenesis and translation, glycolysis, amino acid metabolism, stress response, and detoxification showed an increased expression in the parasitic mycelium. These data indicate a strong shift in gene expression in rust fungi between germination and the biotrophic stage of development.
© 2005 Published by Elsevier Inc.

Keywords: *Vicia faba*; Broad bean rust; EST; Biotrophy; Haustorium; cDNA library

1. Introduction

With more than 7000 described species, rust fungi (Uredinales, Basidiomycota) belong to the largest group of plant pathogenic fungi. Among their host plants are many important crops, such as cereal grasses, coffee, and grain legumes, which can suffer serious yield losses from rust disease. In addition to their economic importance, rust fungi are particularly interesting because of their complex life cycle and the specialised infection structures. A great number of cytological studies have revealed details about spore attachment, germination, appressorium formation over host stomata, and host invasion (reviewed by Hahn, 2000). Within the host tissue, the dikaryotic mycelium grows with intercellular hyphae and haustorial mother cells which give rise to haustoria that develop inside living plant cells. Haustoria are believed to be essential for crucial aspects of biotrophic pathogenesis of rust fungi, such as nutrient uptake, vitamin biosynthesis, and host defense suppression (Voegele and Mendgen, 2003). Rust fungi are known as obligate biotrophic organisms, and although one of them, *Puccinia graminis* f.sp. *tritici*, can be grown in axenic culture for a limited time (Fasters et al., 1993), no stable transformation system is available for rust fungi. Gene cloning and expression studies have led to the isolation of an infection structure-specific gene in *Uromyces appendiculatus* (Bhairi et al., 1989), and of several genes that show strong expression in germinated uredospores of *Puccinia graminis* (Liu et al., 1993). Analysis of differentially expressed genes from

* Corresponding author. Fax: +49 631 2054716.
E-mail address: hahn@rhrk.uni-kl.de (M. Hahn).
URL: http://www.uni-kl.de/FB-Biologie/AG-Hahn/ (M. Hahn).

Konstanzer Online-Publikations-System (KOPS)
URL: http://www.ub.uni-konstanz.de/kops/volltexte/2007/3764/
URN: http://nbn-resolving.de/urn:nbn:de:bsz:352-opus-37647

Puccinia triticina-infected wheat leaves resulted in the isolation of several fungal genes that are activated during parasitic growth (Thara et al., 2003; Zhang et al., 2003). A systematic approach towards the identification of biotrophy-related genes has been performed with the broad bean rust *Uromyces fabae*. Based on a protocol for the preparative isolation of haustoria from rust-infected leaves, a haustorium-specific cDNA library was constructed (Hahn and Mendgen, 1992; Hahn and Mendgen, 1997). Differential screening of this library led to the identification of about 30 genes (*PIG*s: in planta induced genes) that are up-regulated during parasitic growth, showing highest transcript levels in haustoria and rust-infected leaves. Three *PIG*s were found to encode nutrient transporters, which are probably involved in the uptake of hexose sugars and amino acids from the infected host cells into haustoria (Hahn et al., 1997; Struck et al., 2002; Voegele et al., 2001). Taken together, this data supported the idea that rust haustoria perform essential metabolic functions in the parasitic mycelium, including nutrient uptake and vitamin biosynthesis (Mendgen and Hahn, 2002).

In this paper, the analysis of about 1000 ESTs from the *U. fabae* haustorium cDNA library is presented. Microarray hybridisation studies revealed in planta-induced expression of a large portion of the analysed genes and provided further insights into the molecular basis of pathogenic differentiation in rust fungi.

2. Materials and methods

2.1. Sequence analysis and database search

Construction of a bacteriophage λgt10 haustorium-specific cDNA library from *U. fabae* (race I_2) is described in Hahn and Mendgen (1997). Individual plaques of the non-amplified library, containing the cDNAs inserted as *Eco*RI fragments, were used for PCR amplification, using the vector primers gt10R (CTTATGAGTATTTCTTCCAGGG TA) and gt10F (GAGCAAGTTCAGCCTGG). Single pass sequencing of the purified PCR fragments was done with primer gt10R; some clones were also sequenced with gt10F. Sequencing was performed by GATC Biotech AG (Konstanz, Germany). Assembly of individual sequences (ESTs) into overlapping contigs was done using the 'Seqman' module of the Lasergene software package (DNAstar, Madison, WI, USA). The settings for contig assembly were 12 nucleotide minimal match size and 75% minimum match. Afterwards, the contigs were manually checked to disconnect inadvertently matched sequences. Comparisons of the ESTs with protein sequences in the public databases were performed using the gapped BlastX algorithm (Altschul et al., 1997). Similarities were classified as hits indicating significant homology when the expected *E* value was lower than 10^{-5}. In few cases, clones with interesting similarities but *E* values higher than 10^{-5} were included.

2.2. Nucleic acid manipulations

Germination of *U. fabae* uredospores on polyethylene sheets and cultivation of *Vicia faba* plants were done as described (Hahn and Mendgen, 1997). To obtain maximal density of infection, leaves were brush-inoculated with uredospores mixed with double amount of talcum. RNA isolation from germinated spores (4–6 h old) and from rust-infected *V. faba* leaves (6 d.p.i.) was done using the RNAeasy kit (Qiagen, Hilden, Germany). RT-PCR experiments were performed with MuLV reverse transcriptase, using oligo(dT) or a gene-specific oligonucleotide as a primer (MBI Fermentas, AB, Vilnius, Lithuania), followed by PCR with the cDNAs and appropriate primers in a separate tube.

DNA isolation from germinated spores was done as described (Hahn and Mendgen, 1997). Total nucleic acids from germinated spores were isolated in the same way, except that RNase treatments were omitted. Treatments of nucleic acids with varying concentrations of RNase A were performed in 5 mM Tris–HCl, pH 8.0, and 0.5 mM EDTA, for 30 min at 37 °C.

2.3. Microarray hybridisation

For microarray hybridisation, PCR amplified and purified *U. fabae* haustorium cDNAs were dissolved at a concentration of 300 ng/μl in 3× SSC, and spotted in duplicate onto Nexterion slides A (SCHOTT Jenaer Glas GmbH, Jena, Germany), using a SpotArray 24 Microarray Printing System (PerkinElmer Life Sciences, Boston, USA). Printed microarrays were fixed with a UV cross linker at 600 mJ. Double-stranded cDNA on the slides was denatured in 0.1% sodium dodecyl sulfate for 30 s, followed by boiling water for 3 min and 70% ethanol for 2 min. Hybridisation was performed with Cy3- and Cy5-labelled cDNA, obtained from total RNA using the LabelStar Array Kit (Qiagen, Hilden, Germany). The dye-labelled cDNA from rust germlings was derived from RNA which had been pooled from three independent preparations of uredospores germinated for 4–6 h either on polyethylene sheets or submersed in water with stirring. Hybridisations were performed with three biological replicates of the infected leaf sample, and a dye swap was done in each experiment. The labelled probes were added to hybridisation buffer containing 5× SSC, 1% bovine serum albumin, 0.1% sodium dodecyl sulfate, and 0.01% salmon sperm DNA. Hybridisation was conducted at 60 °C overnight. After hybridisation, slides were washed for 5 min in 2× SSC at 42 °C, for 1 min in 0.2× SSC, and for 5 s in 0.05× SSC, both times at room temperature. Slides were dried by centrifugation (5 min, 200*g*), and scanned with a ScanArray 4000 Microarray Analysis System (PerkinElmer Life Sciences, Boston, USA) to visualise the hybridisation images.

Signal intensity and ratios were calculated using ScanArray Express 2.1 software (PerkinElmer Life Sciences, Boston, USA). In a first step, cDNA spots with signals lower than the average background plus the double standard deviation of the background were excluded from further analysis. From

the remainder, spots with significant intensity values were selected by the SAM software (Stanford University, Stanford, USA), with a false discover rate (FDR) value of 0.0019. Expression ratios calculated as Cy5/Cy3 signals were normalised using the LOWESS (Locally Weighted Scatter Plot Smoother) method in the Array Informatics software package. The significance of the expression ratios shown in Tables 1 and 2 was estimated using the SAM software, and found to be highly significant ($P < 0.01$ in most cases).

2.4. RNA dot blot hybridisation experiments

Total RNA samples in concentrations of 0.3 and 1.0 μg/ml were incubated at 65 °C for 5 min, and spotted onto positively charged nylon membranes (Carl Roth GmbH, Karlsruhe, Germany). Radioactive hybridisation was carried out at 65 °C, in a buffer system described by Church and Gilbert (1984). As ^{32}P-labelled hybridisation probe, a 324 bp PCR fragment covering the 5.8S rRNA-encoding region of *U. fabae* was used.

3. Results

3.1. EST sequencing

A total of 1017 EST sequences with satisfying quality (sequence reads with less than 1% ambiguous base calls) were generated from a previously constructed haustorium-specific cDNA library of the broad bean rust fungus *U. fabae* (Hahn and Mendgen, 1997). Redundant sequences were merged into 530 contigs. In the following each contig is referred to as one gene, although it cannot be excluded that a few contigs represent non-overlapping portions of the same gene. Contig sequences have been deposited in the NCBI dbEST database (Accession Nos. DR010180–DR010694). To identify genes with protein coding regions that are similar to known proteins, contig sequences were subjected to BlastX searches. Of the 1017 sequenced clones, 554 (54.4%) did not yield significant hits ($E > e^{-05}$); 404 (39.7%) clones matched with proteins of known function, and 59 (5.8%) with proteins of unknown function. Of the 530 contigs, 277 (52.2%) did not reveal significant hits; 215 (40.6%) were similar to proteins of known function, and 38 (7.2%) contigs similar to proteins of unknown function. Among the genes encoding open reading frames similar to proteins of known function, best hits were usually found with sequences from basidiomycetes (*Cryptococcus neoformans* and *Ustilago maydis*) and ascomycetes (e.g., *Schizosaccharomyces pombe*).

In Fig. 1, a functional classification of the contigs based on their sequence similarities to known genes (proteins) is shown. As expected, genes involved in various metabolic pathways are present in the haustorial cDNA library, with

Table 1
Expression levels of *U. fabae* genes showing the strongest up-regulation in rust-infected leaves vs. germinated uredospores

Clone identifier (Accession)	Similarity (Accession)	*E* value	Expression ratio[a]	Relative expression[b]
Uf091 (DR010269)	Unknown	—	194.0	6.4
Uf419 (DR010597)	Unknown	—	54.2	1.2
THI1 (O00057)	*PIG1*; THI1p thiamine biosynth. enzyme (O00057) (Sohn et al., 2000)	0.0[c]	53.9	5.6
MAD1 (O00058)	*PIG8*; MAD1p mannitol dehydrogenase (O00058) (Voegele et al., 2005)	0.0[c]	49.5	1.9
Uf010 (DR010189)	*PIG6*; unknown	—	46.9	2.4
Uf022 (DR010200)	*PIG13*; metallothionein	3.1[d]	44.4	9.4
Uf018 (DR010196)	*PIG24*; unknown	—	28.5	2.6
Uf011 (DR010190)	Unknown	—	25.1	0.1
Uf003 (DR010182)	*PIG3*; unknown	—	24.9	5.3
Uf436 (DR010614)	Triosephosphate isomerase [*Aspergillus nidulans*] (EAA58299)	7e−32	24.9	1.5
PIG11 (AAB39879)	*PIG11*; metallothionein [*U. fabae*] (AAB39879)	4e−08	24.7	16.6
Uf101 (DR010279)	Glutamine synthetase [*Agaricus bisporus*] (CAA73235)	9e−73	24.7	0.2
Uf035 (DR010213)	Unknown	—	23.9	2.2
Uf103 (DR010281)	Unknown	—	22.1	0.1
Uf016 (DR010194)	Unknown	—	20.4	0.6
Uf058 (DR010236)	Manganese superoxide dismutase [*Phanerochaete chrysosporium*] (AAK82369)	2e−27	17.8	1.0
Uf006 (DR010185)	*PIG22*; unknown	—	25.3	1.2
Uf002 (DR010181)	*PIG5*; unknown	—	14.4	8.4
Uf134 (DR010312)	Unknown	—	13.7	0.1
Uf470 (DR010648)	Unknown	—	13.6	2.4
THI2p (CAB59856)	*PIG4*; THI2p thiamine biosynth. enzyme (CAB59856) (Sohn et al., 2000)	0.0[c]	13.5	1.9
Uf124 (DR010302)	Unknown	—	12.0	0.4
Uf244 (DR010422)	Unknown	—	11.2	2.7
HXT1 (CAC41332)	HXT1p [*U. fabae*] (CAC41332) (Voegele et al., 2001)	0.0[c]	10.1	1.0
Uf053 (DR010231)	Regulatory protein cys-3 [*N. crassa*] (CAB98237)	8e−16	9.9	1.6

[a] Ratio of expression in infected leaves vs. expression in germlings.
[b] Expression data relative to expression of β-tubulin gene (AJ311552).
[c] Function confirmed.
[d] Proposed function based on structural properties despite high *E* value.

Table 2
Expression levels of *U. fabae* genes grouped according to their proposed functions

Clone identifier (Accession)	No. of ESTs	Similarity (Accession)	*E* value	Expression ratio	Relative expression
Amino acid metabolism					
Uf072 (DR010250)	2	Imidazolglycerolphosphate hydratase [*Phaffia rhodozyma*] (AAD14685)	2e−61	0.5	0.1
Uf073 (DR010251)	2	Δ1-pyrroline-5-carboxylate reductase [*S. pombe*] (NP_594706)	1e−63	0.3	0.1
Uf048 (DR010226)	3	4-Aminobutyrate aminotransferase [*U. maydis*] (EAK82039)	9e−35	5.9	0.6
Uf180 (DR010358)	1	Saccharopine reductase [*Penicillium chrysogenum*] (CAC87475)	5e−52	1.3	0.7
Uf101 (DR010279)	2	Glutamine synthetase [*A. bisporus*] (CAA73235)	9e−73	24.7	0.2
Uf104 (DR010282)	2	Homoserine dehydrogenase [*C. neoformans*] (AAK83370)	6e−29	1.6	0.8
Uf293 (DR010471)	1	Threonine synthase [*S. cerevisiae*] (CAA35157)	5e−10	0.9	0.2
Uf126 (DR010304)	2	Prephenate dehydrogenase [*C. neoformans*] (AAW46400)	3e−56	0.8	0.2
Uf067 (DR010245)	3	Adenosylhomocysteinase [*C. neoformans*] (AAW43030)	3e−63	1.8	0.8
Uf484 (DR010662)	1	Δ1−pyrroline-5-carboxylate dehydrogenase [*A. bisporus*] (CAA64836)	9e−60	5.3	0.6
Nucleotide metabolism					
Uf156 (DR010334)	1	Ribonuclease [*Trichoderma viride*] (AAB21597)	2e−06	0.1	0.3
Uf078 (DR010256)	1	Uracil phosphoribosyltransferase [*C. neoformans*] (AAW43557)	7e−53	0.6	0.2
Uf157 (DR010335)	1	Uracil phosphoribosyltransferase [*C. neoformans*] (AAW43567)	6e−35	0.4	0.5
Uf203 (DR010381)	1	Guanylate kinase [*S. cerevisiae*] (AAA34657)	1e−45	0.2	0.1
Uf240 (DR010418)	1	Nucleoside-diphosphate kinase [*C. neoformans*] (AAW43656)	6e−54	0.7	0.7
Uf297 (DR010475)	1	Phosphoribosyl-ATP diphosphatase [*C. neoformans*] (AAW42514)	1e−14	1.4	0.1
C-compound and carbohydrate metabolism					
Uf005 (DR010184)	17	*PIG15* Trehalose-phosphate synthase [*S. pombe*] (NP_594975)	1e−07	2.7	0.5
MAD1 (AAB39878)	13	*PIG8* MAD1p Mannitol dehydrogenase [*U. fabae*] (AAB39878)	0.0	49.5	1.9
ARD1 (AJ809335)	6	ARD1p. Arabitol dehydrogenase [*U. fabae*] (AJ809335)	0.0	0.4	0.2
BGL1 (CAE01320)	1	BGL1p Beta-glucosidase [*U. fabae*] (CAE01320)	0.0	n.d.	n.d.
Uf139 (DR010317)	2	β-Fructofuranosidase (invertase) [*Aspergillus niger*] (JC7658)	1e−17	0.6	1.4
Uf008 (DR010187)	10	*PIG18* Chitinase [*P. triticina*] (AAP42832)	e−132	0.3	0.7
Uf471 (DR010649)	1	Glutamine:fructose-6-phosphate amidotransferase [*Volvariella volvacea*] (AAT75220)	1e−99	0.4	0.2
Lipid, fatty acid, and isoprenoid metabolism					
Uf149 (DR010327)	1	Long chain fatty acid elongation enzyme [*Mortierella alpina*] (AAF71789)	4e−46	0.3	0.5
Uf154 (DR010332)	1	Acetyl-CoA acetyltransferase [*C. neoformans*] (AAW42410)	1e−51	3.9	1.2
Uf255 (DR010433)	1	3-Oxoacyl-(acyl carrier protein) reductase [*Sulfolobus solfataricus*] (NP_343661)	3e−19	4.1	0.6
Uf338 (DR010516)	1	Farnesyldiphosphate synthetase [*Kluyveromyces lactis*] (CAA53614)	3e−47	1.3	0.3
Uf363 (DR010541)	1	Triacylglycerol lipase [*C. neoformans*] (AAW42663)	4e−31	0.3	0.1
Uf474 (DR010652)	1	Acyl carrier protein [*C. neoformans*] (AAW42804)	4e−26	1.9	1.2
Uf480 (DR010658)	1	Phospholipid:diacylglycerol acyltransferase [*C. neoformans*] (AAW46497)	3e−33	n.d.	n.d.
Metabolism of vitamins, cofactors, and prosthetic groups					
THI1 (AAB39877)	36	*PIG1* THI1p Thiamine biosynthesis enzyme [*U. fabae*] (AAB39877)	0.0	53.9	5.6
THI2 (CAB59856)	17	*PIG4* THI2p Thiamine biosynthesis enzyme [*U. fabae*] (CAB59856)	0.0	13.5	1.9
Uf121 (DR010299)	2	*PIG32* Pyridoxine biosynthesis enzyme [*Chloroflexus aurantiacus*] (ZP_00358278)	9e−78	n.d.	n.d.
Glycolysis					
Uf259 (DR010437)	1	Glucose-6-phosphate isomerase [*C. neoformans*] (AAW41921)	9e−86	0.5	0.4
Uf045 (DR010223)	3	Fructose-bisphosphate aldolase [*S. pombe*] (P36580)	e−126	1.6	0.4
Uf436 (DR010614)	1	Triosephosphate isomerase [*A. nidulans*] (EAA58299)	7e−32	24.9	1.5
Uf206 (DR010384)	1	3-Phosphoglycerate kinase [*Yarrowia lipolytica*] (AAC37504)	1e−57	2.9	0.8
Uf098 (DR010276)	2	Phosphoglycerate mutase [*Bradyrhizobium japonicum*] (NP_767326)	4e−44	1.7	2.0
Uf027 (DR010205)	5	Glyceraldehyde-3-phosphate dehydrogenase [*C. curvatus*] (Q9Y796)	e−118	4.4	1.5
Uf028 (DR010206)	5	Phosphopyruvate hydratase [*C. neoformans*] (AAW42072)	e−167	1.2	0.8
Uf146 (DR010324)	1	Pyruvate kinase [*A. bisporus*] (CAA66194)	2e−76	1.6	0.3
Pyruvate dehydrogenase complex					
Uf352 (DR010530)	1	Pyruvate dehydrogenase kinase [*S. pombe*] (NP_593879.1)	6e−23	1.6	0.2
Uf387 (DR010565)	1	Pyruvate dehydrogenase kinase [*Arabidopsis thaliana*] (CAA07447)	4e−07	1.1	0.2
Uf456 (DR010634)	1	Pyruvate dehydrogenase β subunit, mitochondrial [*C. neoformans*] (AAW46579)	1e−46	0.5	0.1
Uf219 (DR010397)	1	Dihydrolipoyllysine-residue acetyltransferase [*C. neoformans*] (AAW43137)	7e−35	1.3	0.2
Tricarboxylic-acid pathway					
SDH2 (CAE02642)	1	SDH2p Succinate dehydrogenase [*U. fabae*] (CAE02642)	4e−58	n.d.	n.d.
Uf189 (DR010367)	1	Fumarate hydratase [*Escherichia coli*] (AAN80463)	2e−26	0.4	0.2
Uf024 (DR010202)	6	Malate dehydrogenase [*C. neoformans*] (AAW44706)	4e−92	4.8	0.4
Uf362 (DR010540)	1	Malate dehydrogenase (oxaloacetate-decarboxylating) [*C. neoformans*] (AAW47024)	7e−50	n.d.	n.d.
Uf019 (DR010197)	7	Malate dehydrogenase [*Paracoccidioides brasiliensis*] (AAP37966)	e−110	2.0	0.7
Uf342 (DR010520)	1	Oxoglutarate dehydrogenase (succinyl-transferring) [*C. neoformans*] (AAW41534)	1e−36	3.0	0.8

(*continued on next page*)

Table 2 (*continued*)

Clone identifier (Accession)	No. of ESTs	Similarity (Accession)	*E* value	Expression ratio	Relative expression
Electron transport and membrane-associated energy conservation/respiration					
Uf172 (DR010350)	1	Ubiquinol-cytochrome *c* reductase iron–sulphur subunit [*S. pombe*] (NP_595941)	7e−71	0.6	0.2
Uf302 (DR010480)	1	NADH-ubiquinone oxidoreductase 19.3 kDa subunit [*N. crassa*] (CAF06152)	2e−52	0.4	0.2
Uf358 (DR010536)	1	NADH-ubiquinone oxidoreductase 21.3 kDa subunit [*N. crassa*] (P19968)	9e−09	1.4	2.5
Uf284 (DR010462)	1	NADH-ubiquinone oxidoreductase 30.4 kDa subunit [*N. crassa*] (P23710)	2e−26	0.5	0.3
Uf299 (DR010477)	1	NADH dehydrogenase subunit 5 [*C. neoformans*] (AAN37584)	1e−53	0.9	0.1
Uf252 (DR010430)	1	Apocytochrome *b* [*Rhizopus oryzae*] (AAW49472)	1e−79	0.5	0.7
Uf176 (DR010354)	1	Cytochrome *c* [*Canis familiaris*] (P00011)	1e−33	0.2	0.6
Uf388 (DR010566)	1	Cytochrome *c* oxidase subunit 1 [*Crinipellis perniciosa*] (YP_025835)	6e−71	0.6	0.3
Uf291 (DR010469)	1	Cytochrome *c* oxidase subunit V [*A. niger*] (CAA10609)	5e−24	n.d.	n.d.
Uf243 DR010421)	1	Cytochrome *c* oxidase [*C. neoformans*] (AAW44622)	2e−09	1.7	1.1
Uf037 (DR010215)	3	ATP synthase, subunit 4 [*C. neoformans*] (AAW42110)	1e−48	0.5	3.5
Uf097 (DR010275)	2	ATP synthase α chain [*C. neoformans*] (AAW44019)	e−141	n.d.	n.d.
Uf065 (DR010243)	4	ATP synthase β chain, mitochondrial precursor [*S. pombe*] (NP_593151)	2e−80	2.0	2.3
Uf036 (DR010214)	4	ATP synthase γ chain, mitochondrial precursor [*C. neoformans*] (AAW43492)	1e−46	1.6	0.2
Uf055 (DR010233)	3	ATP synthase oligomycin sensitivity conferring protein [*M. grisea*] (AAW69347)	1e−30	0.8	0.4
Uf500 (DR010678)	1	ATP-synthase δ subunit [*A. bisporus*] (CAB04785)	1e−38	0.9	1.0
Ribosome biogenesis					
Uf360 (DR010538)	1	40S ribosomal protein S5 [*A. nidulans*] (EAA65673)	1e−61	3.0	2.2
Uf063 (DR010241)	4	40S ribosomal protein S6 [*Pseudopleuronectes americanus*] (AAT01908)	8e−14	0.3	1.7
Uf148 (DR010326)	1	40S ribosomal protein S23 [*N. crassa*] (Q9HE74)	6e−68	1.9	1.4
Uf150 (DR010328)	1	40S ribosomal protein S28 [*Sus scrofa*] (AAS55896)	3e−22	7.3	1.9
Uf382 (DR010560)	1	60S ribosomal protein L7 [*N. crassa*] (Q7SBD5)	9e−87	n.d.	n.d.
Uf478 (DR010656)	1	60s ribosomal protein L7a (L8) [*S. pombe*] (NP_595832)	3e−51	9.4	2.0
Uf349 (DR010527)	1	60S ribosomal protein L8 [*Xenopus laevis*] (P41116)	e−100	1.4	1.1
Uf283 (DR010461)	1	60S ribosomal protein L9 [*S. cerevisiae*] (P31334)	2e−31	0.9	0.1
Uf282 (DR010460)	1	60S ribosomal protein L14-B [*S. cerevisiae*] (P38754)	1e−27	2.4	2.2
Uf462 (DR010640)	1	60S ribosomal protein L15-2 [*Dictyostelium discoideum*] (AAO51334)	2e−61	2.2	2.7
Uf093 (DR010271)	2	60S ribosomal protein L24 [*C. neoformans*] (AAW44673)	4e−31	2.4	2.5
Uf165 (DR010343)	1	60S ribosomal protein L25 [*Puccinia graminis f. sp. avenae*] (P51997)	3e−77	2.9	1.9
Uf237 (DR010415)	1	60S ribosomal protein L32 [*S. pombe*] (NP_594182)	2e−45	2.9	4.1
Uf202 (DR010380)	1	60S ribosomal protein RL36_TRIHM [*Gibberella zeae*] (EAA68099)	5e−33	3.0	0.4
Uf371 (DR010549)	1	60S ribosomal protein L44 [*Coprinopsis cinerea*] (Q9UWE4)	2e−53	6.5	1.5
Uf080 (DR010258)	1	Ribosomal protein (processing of 20S pre-rRNA) [*C. neoformans*] (AAW47003)	8e−42	0.4	0.2
Uf380 (DR010558)	1	Ribosomal protein L13A [*Xanthophyllomyces dendrorhous*] (CAC24570)	4e−70	1.3	0.9
Uf422 (DR010600)	1	Ribosomal protein L35 [*C. neoformans*] (AAW41280)	2e−38	2.4	1.5
Uf120 (DR010298)	2	Ribosomal protein S11 [*C. neoformans*] (AAW41172)	2e−51	2.6	1.2
Uf406 (DR010584)	1	S-phase specific ribosomal protein cyc07 [*Lentinula edodes*] (BAD11816)	2e−45	5.0	1.6
Translation					
Uf114 (DR010292)	2	Eukaryotic translation initiation factor 3 subunit 2 [*S. pombe*] (NP_594958)	2e−60	1.7	0.4
Uf322 (DR010500)	1	Elongation factor 2 [*S. pombe*] (NP_593975)	7e−40	2.1	1.7
Uf137 (DR010315)	2	Elongation factor 1 β [*S. pombe*] (NP_588303)	1e−40	n.d.	n.d.
Uf503 (DR010681)	1	Translation initiation factor 2 β subunit [*S. pombe*] (NP_593772)	7e−61	1.3	0.2
Aminoacyl-tRNA-synthetases					
Uf199 (DR010377)	1	Threonyl-tRNA synthetase, cytoplasmic [*S. cerevisiae*] (NP_116578)	4e−54	0.3	0.2
Uf445 (DR010623)	1	Seryl-tRNA synthetase, cytoplasmic [*S. pombe*] (O14018)	8e−32	0.9	0.2
Cellular transport and transport facilitation					
HXT1 (CAC41332)	3	HXT1p hexose transporter [*U. fabae*] (CAC41332)	7e−80	10.1	0.2
Uf249 (DR010427)	1	UDP-galactose transporter [*S. pombe*] (BAA77219)	7e−27	2.1	0.2
AAT2 (CAC67419)	4	*PIG2* AAT2p putative amino acid transporter [*U. fabae*] (CAC67419)	0.0	1.0	2.1
AAT1 (CAC67419)	2	*PIG27* AAT1p amino acid transporter [*U. fabae*] (CAC67419)	4e−77	1.1	0.2
AAT3 (CAF32328)	1	AAT3p; amino acid transporter [*U. fabae*] (CAF32328)	e−134	0.7	0.1
Uf145 (DR010323)	1	Peptide transporter MTD1 [*Schizophyllum commune*] (AAF26618)	1e−11	n.d.	n.d.
Uf040 (DR010218)	4	ATP:ADP antiporter [*C. neoformans*] (AAW46785)	2e−85	2.4	3.0
Uf196 (DR010374)	1	Na^+/K^+-exchanging ATPase [*Blastocladiella emersonii*] (T43025)	4e−21	0.1	0.3
PMA1 (CAA05841)	2	PMA1p Plasma membrane (H^+) ATPase [*U. fabae*] (CAA05841)	e−149	0.1	0.4
Uf175 (DR010353)	1	Organic acid transporter [*C. neoformans*] (AAW42240)	6e−39	0.7	0.2
Uf366 (DR010544)	1	Glycerol transporter [*C. neoformans*] (AAW43957)	1e−71	0.4	0.1
Uf042 (DR010220)	4	Integral membrane transporter protein [*Homo sapiens*] (CAB81951)	1e−06	2.3	0.4
Uf278 (DR010456)	1	Voltage-dependent ion-selective channel [*C. neoformans*] (AAW42497)	2e−17	n.d.	n.d.
Uf066 (DR010244)	1	Possible transporter-like protein [*A. fumigatus*] (CAF32106)	1e−13	1.9	0.6

Table 2 (*continued*)

Clone identifier (Accession)	No. of ESTs	Similarity (Accession)	*E* value	Expression ratio	Relative expression
Cytoskeleton					
Uf051 (DR010229)	3	Myosin tail region-interacting protein MTI1 [*S. cerevisiae*] (P47068)	2e−06	1.7	0.2
TBB1 (CAC83953)	1	TBB1p β Tubulin [*U. fabae*] (CAC83953)	1e−64	1.1	1.0
Uf393 (DR010571)	1	Actin binding protein [*Saccharomyces exiguus*] (CAA52156)	4e−15	0.4	0.1
Stress response					
Uf105 (DR010283)	2	Heat shock protein 90 [*Cryptococcus bacillisporus*] (AAN76524)	8e−19	1.0	1.2
Uf274 (DR010452)	1	Small heat shock protein [*Paxillus filamentosus*] (AAT91263)	9e−21	n.d.	n.d.
Uf130 (DR010308)	2	Heat shock protein [*C. neoformans*] (AAW41904)	2e−80	5.8	0.6
Uf449 (DR010627)	1	Heat shock protein 78 [*Leptosphaeria maculans*] (AAO49455)	2e−25	0.6	0.2
PIG11 (AAB39879)	8	*PIG11* Metallothionein [*U. fabae*] (AAB39879)	0.0	24.7	16.6
Uf022 (DR010200)	6	*PIG13* Metallothionein [*Mytilus galloprovincialis*] (AAT72935.1)	3.1	44.4	9.4
PIG28 (AAB39880)	4	*PIG28* Peptidyl prolyl *cis*/*trans*-isomerase [*S. pombe*]	0.0	8.7	7.9
Detoxification					
PIG16 (AAB39881)	1	*PIG16* Cytochrome P450 monooxygenase [*Aspergillus parasiticus*]	0.0	7.6	0.3
Uf138 (DR010316)	2	Phenol 2-monooxygenase [*N. crassa*] (CAF06102)	3e−19	1.6	0.2
Uf434 (DR010612)	1	Glutamate-cysteine ligase [*C. neoformans*] (AAW47039)	4e−78	0.5	0.1
Uf468 (DR010646)	1	Glutathione *S*-transferase kappa 1 [*H. sapiens*] (EAL23783)	5e−11	0.5	0.1
Uf058 (DR010236)	2	Manganese superoxide dismutase [*P. chrysosporium*] (AAK82369)	2e−27	17.8	1.0
Uf197 (DR010375)	1	Thioredoxin peroxidase 1 [*Lycopersicon esculentum*] (AAP34571.1)	1e−33	2.6	2.2
Uf092 (DR010270)	2	Peroxidase [*Galactomyces geotrichum*] (BAA77283)	9e−05	9.8	0.2
Uf443 (DR010621)	1	Mitochondrial cytochrome c peroxidase [*C. neoformans*] (AAR20479)	4e−23	7.4	0.2
Viral proteins					
Uf239 (DR010417)	1	RNA replicase [Cucumber green mottle mosaic virus] (BAA87615)	4e−13	0.5	0.7
Uf116 (DR010294)	2	Replicase large component [Cucumber fruit mottle mosaic virus] (AAG42815)	2e−26	1.3	0.6
Uf128 (DR010306)	2	RNA replicase [Cucumber green mottle mosaic virus] (AM02966)	2e−08	0.5	1.5

Functional classification was performed according to the FunCat annotation scheme (Ruepp et al., 2004). The number of EST sequences for each gene (contig) are indicated. For further explanations, see Table 1.

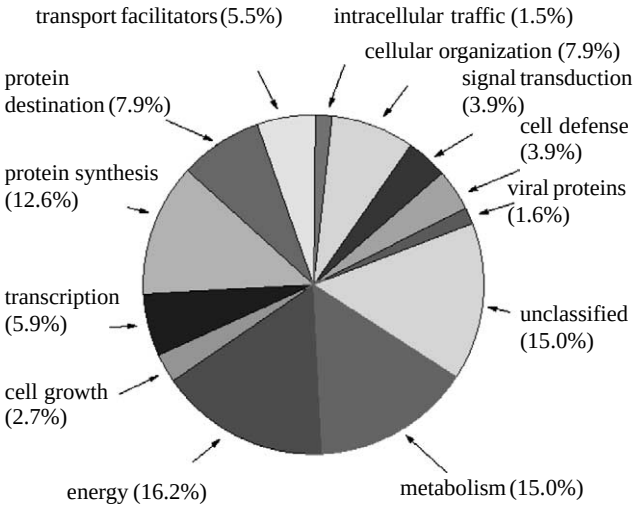

Fig. 1. Functional classification of 253 contigs from the haustorium-specific cDNA library of *U. fabae* showing significant similarity (*E* value < 10^{-5}) to proteins in public databases.

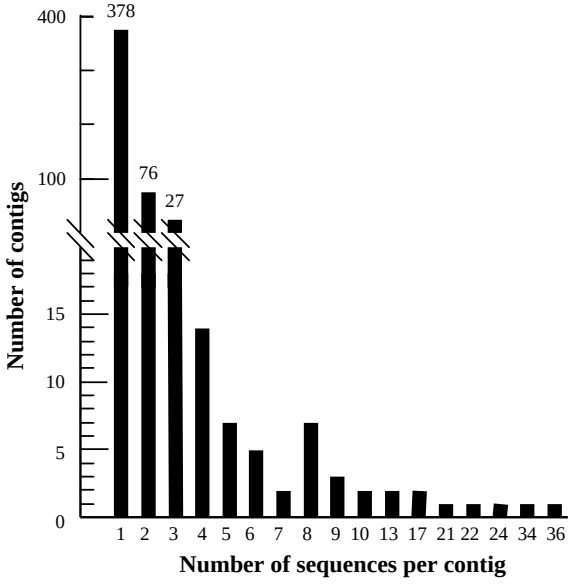

Fig. 2. Frequency distribution of sequences from the EST library belonging to the same contig (gene).

highest proportions of genes involved in energy production, metabolism, and protein synthesis. Interestingly, we found three ESTs encoding virus-like genes (see below). Because EST sequencing was performed with a non-amplified cDNA library, the frequency of occurrence of the ESTs was expected to provide a rough estimate of the abundance of the corresponding mRNAs in haustoria. As shown in Fig. 2, 378 of the 530 contigs originated from unique ESTs (singletons), while 152 contigs were represented by more than one EST. Several of these contigs were found with unusually high frequency (up to 36 times, i.e., 3.5% of all ESTs). Among the 21 most highly represented contigs (>8 times), 14 corresponded to the in planta induced genes (*PIG*s) described in Hahn and Mendgen (1997), namely:

PIG1 (36x); *PIG5* (24x); *PIG3* (22x); *PIG4*, *PIG15* (17x); *PIG8*, *PIG22* (13x); *PIG14*, *PIG18* (10x); *PIG6*, *PIG7* (9x); *PIG9*, *PIG11*, *PIG12* (8x). This supports our previous observation that a set of genes is induced in haustoria to very high levels.

3.2. Identification of plant virus-like sequences in the genome of U. fabae

Unexpectedly, three contigs were identified that encode virus-like proteins. Interestingly, all three contigs are similar to the same type of viral RNA replicase, as exemplified by the 1648 amino acid cucumber green mottle virus RNA replicase (Fig. 3A). Similar RNA replicases occur in various plant viruses that contain single-stranded (+) RNA genomes, such as tobamoviruses, bromoviruses, and closteroviruses. Several mycoviruses are known from fungi, but only one of them, *Botrytis cinerea* virus X (Accession No. AY055762), showed a low level of similarity to the two contigs *Uf239* and *Uf116*. The partial open reading frames encoded by *Uf239* and *Uf116* show 35% identity to each other, while the similarities of these sequences to corresponding regions of plant virus replicases are around 30% (not shown). *Uf128* showed similarity to a more 5′-located region of the same replicase genes. To check whether the viral-like ESTs are encoded in the *U. fabae* genome, total DNA from *U. fabae* was used as a template for amplification of contig *Uf239*-specific sequences. No product was obtained (data not shown). To detect *Uf239*-specific RNA in *U. fabae*, RT-PCR experiments were performed, using either oligo(dT) or a Uf239-specific oligonucleotide as primers for reverse transcription. *Uf239*-specific sequences were detected in the RNA of germinated spores and rust-infected leaves but not in uninfected *V. faba* leaves (Fig. 3B; data not shown). When the *U. fabae* total DNA preparation was loaded on an agarose gel, we detected several bands in addition to the high molecular weight DNA, the most prominent band with an apparent molecular weight of 5 kb (Fig. 3C). The bands resembled dsRNA known from other fungi, including rust fungi (Zhang et al., 1994). This was confirmed by treating a total nucleic acid preparation from *U. fabae* with varying concentrations of RNase A. It had previously been shown that dsRNA is less susceptible to degradation by RNase A than ssRNA (Khramtsov et al., 1997). In fact, at a concentration of 1 μg/ml RNase A, the bulk of RNA was degraded, while the 5 kb band was still present. At higher concentrations of RNase A, the 5 kb band also disappeared, confirming that it represents dsRNA (Fig. 3D). When the *U. fabae* DNA preparation containing the putative dsRNA was subjected to RT-PCR as described above, no Uf239-specific products were obtained (not shown). These data make it unlikely that the viral EST sequences are encoded in the dsRNA. In summary, these data indicate that *U. fabae* contains several virus-like RNAs.

3.3. Sequence polymorphism of cDNAs

Because haustoria are part of a dikaryotic mycelium, each individual gene is likely to be present in two allelic copies, each copy originating from another nucleus. The availability of redundant sequences in the haustorial cDNA

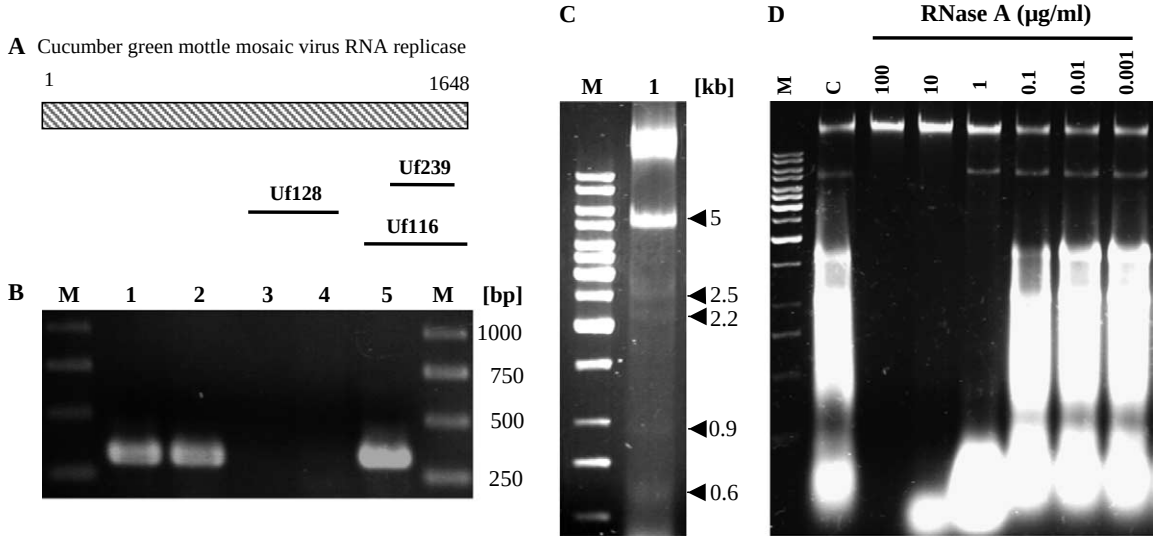

Fig. 3. Evidence for viral RNAs in *U. fabae*. (A) Position of the coding regions of three contigs relative to the cucumber green mottle mosaic virus RNA replicase (Accession No. AAM02966.1). (B) Detection of viral RNAs by RT-PCR. The following samples were subjected to RT-PCR, using oligo(dT) primers for reverse transcription and Uf239-specific primers for PCR: Lane 1, RNA from *U. fabae* germlings; lane 2, RNA from rust-infected *V. faba* leaves. Lane 3, RNA from non-infected *V. faba* leaves. Lane 4, RNase-treated total DNA from *U. fabae*. In lane 5, a 328 bp PCR fragment obtained with Uf239 cDNA was loaded as a control. (C) Stained agarose gel showing total DNA of *U. fabae* (strong band on top of the lane) and several bands representing virus-like dsRNA (arrowheads). M, molecular weight markers. (D) Differential RNase A sensitivity of the 5 kb dsRNA and total ssRNA. In the control (C), a total nucleic acid preparation from *U. fabae* without RNase treatment was loaded. In the other lanes, the nucleic acids were treated with the indicated concentrations of RNase A, before agarose electrophoresis.

library made it possible to check for possible allelic polymorphisms. An example with a high number of polymorphic bases is *PIG11* encoding a putative metallothionein; its 364 bp cDNA contained four bases which were different in the two populations of the *PIG11* EST sequences, as well as a cluster of four bases in the 3′-non-coding region which were missing in one of the *PIG11* alleles. Amongst the eight available ESTs for *PIG11*, four belonged to each of the two polymorphic sequence types. When the sequences of all contigs represented by at least four overlapping ESTs were screened for polymorphisms, taking into account only polymorphic sequence types supported by at least two ESTs, 66 nucleotide positions with sequence variations were identified within a total of 15,283 bp cDNA sequences (0.43%). When the cDNAs were divided into coding and non-coding regions, 15 polymorphic positions (0.17%) were found to be located within the coding regions (open reading frames of >300 bp), and 51 polymorphic positions (0.76%) in the non-coding regions. Although these numbers are derived from the analysis of single pass sequences which might include some sequence errors, the data nevertheless indicate the occurrence of sequence polymorphism. Until more sequence data are available, it is not possible to distinguish whether these polymorphisms are due to allelic variation or to the presence of gene families.

3.4. Microarray hybridisation

To analyse stage-specific gene expression, cDNAs representing 512 contigs were spotted as microarrays onto slides. Hybridisation was performed with Cy3- and Cy5-labelled cDNA probes, which had been synthesised from in vitro germinated uredospores (4–6 h old) and from rust-infected *V. faba* leaves prior to sporulation (6 d.p.i.), respectively. From all cDNAs spotted, 381 (69%) yielded significant hybridisation signals which allowed the calculation of intensity ratios. For their interpretation, it has to be taken into account that RNA from rust-infected leaves contains a mixture of plant and fungal RNA. To estimate the fraction of rust RNA within the infected leaf RNA sample, we performed dot blot hybridisations using aliquots of the RNA samples which had been used as templates for the labelled cDNA probes used in the microarray hybridisation experiments. As hybridisation probe, a PCR fragment covering the 5.8S rRNA-encoding DNA from *U. fabae* was used. Control experiments confirmed that the probe was specific for rust RNA and did not detect *V. faba* RNA. Quantitative evaluation of the hybridisation data revealed that the RNA samples from infected leaves contained between 40 and 50% of rust RNA (data not shown). Thus, the microarray hybridisation data shown represent a 2- to 2.5-fold underestimation of the expression levels in the parasitic mycelium.

In Fig. 4, a scatter diagram illustrating the intensities and ratios of hybridisation of the spotted DNAs to the dye-labelled cDNAs from rust germlings and infected leaves is

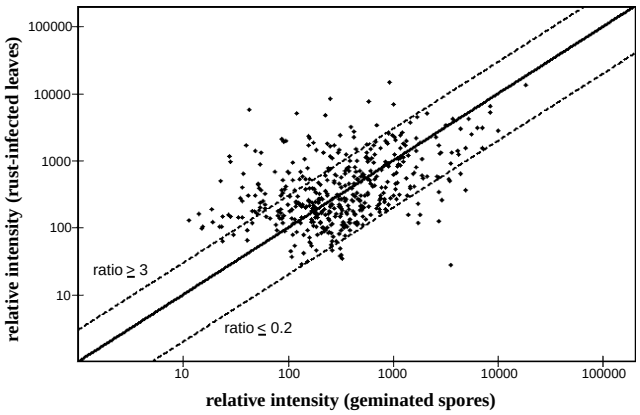

Fig. 4. Scatter plot of the data obtained with 381 *U. fabae* cDNAs after microarray hybridisation with Cy3- and Cy5-labelled cDNAs from germinated spores and rust-infected *V. faba* leaves.

shown. Among the 381 cDNAs that yielded significant expression data, 95 (25%) showed significantly stronger signals (>3-fold; $P < 0.05$) with the probes derived from infected leaves than with the probes from germinated uredospores. If the threshold of induction was reduced to >1.5-fold (due to the reduced content of fungal mycelium in infected leaves, this would still mean at least threefold induction), even 180 (47%) cDNAs could be classified as being induced in the parasitic mycelium as compared to germinated spores. In contrast, only 16 (3.0%) of the cDNAs showed significantly stronger expression in germinated spores.

Twenty-five genes showing the highest ratios of induction (biotrophic mycelium vs. germinated spores) are shown in Table 1. Among these genes are 10 known in planta induced genes (*PIG*s), which had been identified on the basis of differential plaque hybridisation and Northern hybridisation experiments (Hahn and Mendgen, 1997). To provide an estimate of the expression levels of these genes in the parasitic mycelium, their average microarray hybridisation signal intensity was compared to that of the β-tubulin gene which had been shown to be constitutively expressed in different stages of rust development (Wirsel et al., 2004). A large proportion of the strongly induced genes was found to be highly expressed in the biotrophic mycelium, in particular *PIG11*, *PIG13*, and *PIG5* (Table 1). *PIG11* and *PIG13* are interesting because both genes are transcribed into mRNAs of approximately 0.4 kb, and both encode small cystein-rich peptides of 24 and 31 amino acids with similarities to metallothioneins (Hahn and Mendgen, 1997; Fig. 5). When the frequency of occurrence of ESTs in

```
PIG11:              MNPCSSNCSCGASCTCSGCSSHKK
                          ||||::: :|:  ||...
mouse MT1:             MDPNCSCSTGGSCTCTSSCACKNCKCT...
                             ::  || |||:|  ||
PIG13:              MPSGCICKGGCDSACATCQSSCTCSSCKVHH
                      |||||||  |
mouse MT4:     ..(44)CARGCICKGGSDKCSCCP
```

Fig. 5. Similarity of the *PIG11*- and *PIG13*-encoded proteins with mouse metallothioneins MT1 (NP_038630) and MT4 (NP_032657).

the haustorial cDNA library was compared with the microarray hybridisation signal intensities of the corresponding genes in the parasitic mycelium, similar, but not identical, gene expression patterns were obtained. For instance, *PIG1*, *PIG3*, *PIG5*, *PIG6*, *PIG11*, and *PIG13* were among the most highly expressed genes in both cases, while *PIG7*, *PIG14*, and *PIG15* appeared to be much highly expressed in haustoria than in the infected leaf tissue (not shown). For *PIG7* and *PIG15*, a haustorium-specific expression has been recently confirmed on the protein level by immunofluorescence microscopy (Kemen et al., 2005).

In Table 2, hybridisation data for *U. fabae* cDNAs belonging to several major functional categories are summarised. Interestingly, a high proportion of genes that are involved in certain metabolic pathways show significantly higher expression in the biotrophic mycelium than in germinated spores. For instance, 5 out of 10 genes involved in amino acid metabolism, 6 out of 8 genes involved in glycolysis, 16 out of 24 genes encoding ribosomal proteins and translational factors, and 10 out of 15 genes encoding proteins that could be involved in stress response and detoxification are up-regulated by a factor of at least 1.5, without considering the reduced content of fungal RNA in the infected leaves. In contrast, genes belonging to other functional categories, such as nucleotide metabolism and respiration, are not stronger expressed (Table 2; data not shown). Thus, our data do not provide evidence for a general increase in gene expression in *U. fabae* when it enters the biotrophic growth phase.

4. Discussion

This manuscript extends the work by Hahn and Mendgen (1997), describing the results of a systematic search for rust genes involved in pathogenesis. This search was based on: (i) the construction of a haustorium-specific cDNA library, (ii) the generation of EST sequences and analysis for their coding region by database searches, and (iii) the analysis of stage-specific gene expression during parasitic growth. In another study, in planta induced genes of *P. triticina* have been identified in a cDNA library from rust-infected leaves, which had been enriched for fungal genes by suppression subtractive hybridisation (Thara et al., 2003). Among the 26 *P. triticina* genes that were found to be preferentially expressed within the plant, three were similar to *PIG1*, *PIG4*, and *PIG28* of *U. fabae*. This indicates that in different rust fungi, the pattern of gene expression in planta is similar at least in part.

Sequencing of 1017 ESTs revealed almost 50% redundant sequences, which allowed us to condense them into 530 contigs. The abundance of frequently occurring sequences in the haustorial cDNA library was used for an approximate estimate of their expression level in haustoria. Fourteen out of the 21 most highly represented contigs corresponded to *PIG*s described in Hahn and Mendgen (1997). These data confirm our previous observation that in haustoria, some of the most highly expressed genes are in planta induced (Hahn and Mendgen, 1997). More than half of the 530 contigs did not show significant similarity to known genes in the database. This observation is similar to results obtained in EST and complete genomic sequencing projects with other fungi. For instance, of 2676 ESTs clones sequenced from *Blumeria graminis*, 50% did not reveal significant similarities to other genes (Thomas et al., 2001); of the 8177 unique sequences derived from a large scale EST analysis of *Magnaporthe grisea*, only 57% had counterparts in the genome of *Neurospora crassa* (Ebbole et al., 2004).

In the EST library, three contigs were identified that encode proteins similar to viral RNA replicases. The highest similarities of these sequences were found with sequences from plant viruses; only low levels of similarity were observed to the *B. cinerea* virus X. However, the EST sequences clearly originated from *U. fabae*, because they were detected by RT-PCR in RNA from germlings and rust-infected leaves but not from non-infected *V. faba* leaves. According to the microarray data, they are expressed both during germination and in the biotrophic mycelium (Table 2). In agreement to their similarity to RNA viruses, we failed to detect these sequences by PCR using genomic DNA of *U. fabae* as template. This indicates that they occur exclusively as RNA. The majority of fungal viruses (mycoviruses) described consist of dsRNA, such as the hypovirulence-inducing mycoviruses found in *Cryphonectria parasitica* and *Fusarium graminearum* (Chu et al., 2002; Dawe and Nuss, 2001). Nevertheless, ssRNA mycoviruses have also been identified, such as the oyster mushroom virus *Pleurotus ostreatus* (Yu et al., 2003) and the two *B. cinerea* viruses X and F. In rust fungi, a variety of dsRNAs have been identified, e.g., in the line rust *Melampsora lini*, but only little sequence information is available (Zhang et al., 1994). Because we were able to amplify the viral sequences from total rust RNA, but not from the dsRNAs observed in *U. fabae*, they are more likely derived from ssRNA. Taken together, our data indicate that *U. fabae* contains, in addition to several dsRNAs with unknown sequences, at least two novel (+) ssRNA mycoviruses which show low similarities to the *B. cinerea* viruses X and F. Because *U. fabae* race I_2 is fully virulent on its host plant, we conclude that the presence of these different virus-like RNAs does not markedly affect its pathogenicity. Electron microscopic studies with *U. fabae* race I_2 over the last 20 years did not reveal evidence for virus-like particles in the cells (K. Mendgen et al., unpublished observations). It remains to be determined whether the viral RNAs in *U. fabae* are encapsidated.

With the EST clones, a comparative analysis of rust gene expression during germination and during parasitic growth in planta was performed by microarray hybridisation. For 69% of the clones, reproducible hybridisation data were obtained that allowed the calculation of relative ratios of gene expression in the two samples. Remarkably, 95 (25%) of the significantly expressed genes showed at least threefold higher expression in the biotrophic mycelium than in germinated spores. If one considers the relative amount of

fungal mRNA in infected leaves which was determined to be 40–50%, the number of in planta (>3-fold) induced fungal genes rose to 180 (47%). Although the clones were isolated from a haustorium-specific cDNA library and therefore are clearly enriched for in planta induced genes, these results illustrate that gene expression in *U. fabae* changes dramatically between germination and parasitic growth. Among the genes showing the strongest up-regulation in planta are several of the previously identified *PIG*s. Only three of the *PIG*s described in Hahn and Mendgen (1997), namely *PIG17*, *PIG18*, and *PIG23*, were found to be not induced, while one (*PIG10*) was not detectable. Thus, the data obtained with blot hybridisations (Hahn and Mendgen, 1997) and those obtained with microarray hybridisation are similar. However, there was a significant difference in the two studies because the *PIG*s were identified on the basis of their increased expression in haustoria as compared to in vitro grown hyphae (germlings and infection structures), whereas the microarray data compared the gene expression of the *whole* parasitic mycelium with that of germlings. This difference led to different results in some cases, as illustrated by the example of *PIG18*/*Uf008*: Northern hybridisation data revealed a moderate expression of *PIG18* mRNA in germ tubes, the strongest expression in haustoria, and a much lower expression in infected leaves (Fig. 1 in Hahn and Mendgen, 1997). By microarray hybridisation, the mRNA levels of *PIG18* were found to be 3.5-fold higher in germlings than in rust-infected leaves (Table 1), which is in agreement with the Northern data. The gene encoding a putative amino acid transporter (*PIG2*/*AAT2*), which has previously been described to be specifically expressed in haustoria (Hahn et al., 1997), also did not show clearly in planta induced expression in the microarray studies. This is most likely explained by the low level of expression of *PIG2* in germ tubes (which was not detected by Northern analysis; Hahn et al., 1997) and the lack of expression in the intercellular hyphae, which contribute a much greater biomass than haustoria to the total biotrophic mycelium. Other *PIG*s, such as *PIG1* (*THI1*) and *PIG28*, have previously shown to be expressed probably in the whole parasitic mycelium, but not or only very weakly in germlings (Hahn and Mendgen, 1997), and therefore exhibited high ratios of induction in the microarrays.

In addition to the previously identified *PIG*s, the microarray hybridisation data have revealed a large number of new rust genes with strongly induced expression in the parasitic mycelium. Of the 50 most strongly induced genes, 33 (66%) did not match any known genes in the databases, indicating that they might perform specific functions associated with biotrophic growth. It would be of eminent interest to disclose the function of these genes, in order to understand the molecular basis of rust parasitic growth. However, due to the lack of a stable transformation system, this goal will be difficult to achieve.

When the EST clones were grouped into functional categories, several of these groups included a high proportion of genes that are up-regulated in the biotrophic mycelium. This is particularly evident for genes encoding ribosomal proteins. Therefore, rust hyphae seem to have a strongly increased translational activity during in planta growth, as compared to the germination stage. Similarly, genes encoding enzymes involved in glycolysis and amino acid metabolism, as well as thiamine biosynthesis (Sohn et al., 2000) are also more strongly expressed in planta. Whether or not this means a general up-regulation of these metabolic pathways cannot be answered until more comprehensive studies with more or even all genes are available. With regard to the genes involved in amino acid metabolism, those encoding pyrroline-5-carboxylate dehydrogenase (involved in glutamate biosynthesis) and glutamine synthetase indicate that the biosynthesis and interconversion of glutamate and glutamine, and the assimilation of ammonia are important processes during biotrophic growth. It has previously been shown that in *U. fabae*, at least three amino acid permeases are expressed in the biotrophic mycelium. While PIG2p (AAT2p) has an unknown substrate specificity (Hahn et al., 1997), AAT1p (PIG27p) is specific for lysine and histidine (Struck et al., 2002), and AAT3p is a broad specificity amino acid transporter (Struck et al., 2004). Based on the gene expression data for these transporters, amino acid uptake seems to occur both via haustoria and via intercellular hyphae. Subsequently, amino acids probably need to be converted to fulfill the needs for fungal metabolism. Up-regulation of a 4-aminobutyrate (GABA) aminotransferase has also been observed in the biotrophic fungus *Cladosporium fulvum* during infection (Solomon and Oliver, 2002). Low but significant concentrations of GABA have been detected in the apoplast of rust-infected broad bean leaves (Struck et al., 2004). As it has been proposed for *C. fulvum*, GABA might be a significant nitrogen source for biotrophic fungi in general. Taken together, the strong expression changes of genes involved in metabolism are probably a consequence of the fundamentally different nutritional conditions of germinated spores and the parasitic mycelium. In the former stage, the fungus lives exclusively at the expense of the nutrient stores of the uredospores, and these limited resources need to be used as economically as possible. This could explain the relatively low levels of expression of ribosomal proteins; possibly, translation in germinated spores occurs mostly with preformed ribosomes. On the other hand, the biotrophic mycelium receives supply of a variety of host-derived assimilates, including sugars and amino acids, which are used for proliferative growth and later for sporulation. In this stage, a large proportion of hexoses which have been taken up mainly by haustoria via the HXT1p hexose transporter (Voegele et al., 2001) seem to be broken down primarily via the Emden–Meyerhof pathway, to feed energy production. However, a significant portion of the sugars are converted into polyols such as mannitol and arabitol (see below).

Among the newly discovered genes that are strongly up-regulated during parasitic growth, several genes seem to encode proteins involved in stress response Amongst them, *PIG11* and *PIG13* which encode putative metallothioneins

belonging to the three most strongly expressed genes in the parasitic mycelium (data not shown). Metallothioneins have been implicated in various physiological processes, such as binding and detoxification of metals and scavenging of oxygen radicals (Coyle et al., 2002). In *M. grisea*, metallothioneins are highly expressed in all stages of development, and metallothionein 1 (NMT1) was found to be essential for appressorium-mediated penetration of intact leaf surfaces, but not the later stages of pathogenesis (Tucker et al., 2004). Other genes that are predominantly expressed in the biotrophic mycelium might be involved in detoxification of reactive oxygen species, namely a manganese superoxide dismutase and three peroxidases. A Cu–Zn-superoxide dismutase has been described recently to be induced and possibly be involved in antioxidative defense during symbiotic growth in the endomycorrhizal fungus *Gigaspora margarita* (Lanfranco et al., 2005). A possible role in anti-oxidative defense has also been implicated for two enzymes involved in polyol metabolism, namely mannitol dehydrogenase 1 (MDH1p) and arabitol dehydrogenase 1 (ARD1p). Mannitol and arabitol are produced by the parasitic mycelium and released into the apoplast, where they might detoxify reactive oxygen radicals from the host plant (Link et al., 2005,).

In contrast to the large number of genes that are up-regulated during parasitic growth, we identified only 16 genes that are at least fivefold (or two- to threefold, when considering the reduced amount of fungal RNA in the infected leaves sample) higher expressed in germlings than in infected leaves. While the function of most of these genes is unknown, *PMA1* has been previously shown to encode a plasma membrane H^+ ATPase (Struck et al., 1998). Interestingly, the enzyme was found to be significantly more active in membranes isolated from haustoria compared to membranes from germlings (Struck et al., 1996). However, in agreement to the microarray data, Northern blot hybridisation experiments revealed that the *PMA1*-encoding gene was more strongly expressed in germ tubes and in vitro grown rust hyphae than in haustoria and rust-infected leaves (Struck et al., 1998).

The work described in this paper has been done with approximately 5% of all genes from *U. fabae* only, based on the predicted number of approximately 10,000 genes in the completely sequenced genomes of filamentous fungi (Dean et al., 2005). Nevertheless, our data indicate that a considerable reprogramming of gene expression occurs in rust fungi between early stages of development and the parasitic growth phase. Recently, a detailed microarray expression analysis with ESTs from the barley powdery mildew *Erysiphe graminis* f.sp. *tritici* has been published. Similar to our work, it revealed a stage-specific gene expression profile indicating a coordinate regulation of genes encoding enzymes involved in similar metabolic pathways (Both et al., 2005). It is a great challenge to uncover the function of the gene products that are specifically expressed in planta, in particular those proteins that are secreted into the host–parasite interface and which might be important for the establishment and maintenance of the biotrophic interaction.

Acknowledgments

We thank Uta Hempel, Michael Ernst, and Sabine Oldendorf for help with EST sequencing. We are grateful to Ralf Voegele for critically reading the manuscript. This work was supported by the German Science Foundation (DFG; grant Me 523/23).

References

Altschul, S.F., Madden, T.L., Schaffer, A.A., Zhang, J., Zhang, Z., Miller, W., Lipman, D.J., 1997. Gapped BLAST and PSI-BLAST: a new generation of protein database search programs. Nucleic Acids Res. 25, 3389–3402.

Bhairi, S.M., Staples, R.C., Freve, P., Yoder, O.C., 1989. Characterization of an infection structure-specific gene from the rust fungus *Uromyces appendiculatus*. Gene 81, 237–243.

Both, M., Csukai, M., Stumpf, M.P.H., Spanu, P.D., 2005. Gene expression profiles of *Blumeria graminis* indicate dynamic changes to primary metabolism during development of an obligate biotrophic pathogen. Plant Cell 17, 2107–2122.

Chu, Y.M., Jeon, J.J., Yea, S.J., Kim, Y.H., Yun, S.H., Lee, Y.W., Kim, K.H., 2002. Double-stranded RNA mycovirus from *Fusarium graminearum*. Appl. Environ. Microbiol. 68, 2529–2534.

Church, G.M., Gilbert, W., 1984. Genomic sequencing. Proc. Natl. Acad. Sci. USA 81, 1991–1995.

Coyle, P., Philcox, J.C., Carey, L.C., Rofe, A.M., 2002. Metallothionein: the multipurpose protein. Cell. Mol. Life Sci. 59, 627–647.

Dawe, A.L., Nuss, D.L., 2001. Hypoviruses and chestnut blight: exploiting viruses to understand and modulate fungal pathogenesis. Annu. Rev. Genet. 35, 1–29.

Dean, R.A., Talbot, N.J., Ebbole, D.J., Farman, M.L., Mitchell, T.K., Orbach, M.J., Thon, M., Kulkarni, R., Xu, J.R., Pan, H., Read, N.D., Lee, Y.H., Carbone, I., Brown, D., Oh, Y.Y., Donofrio, N., Jeong, J.S., Soanes, D.M., Djonovic, S., Kolomiets, E., Rehmeyer, C., Li, W., Harding, M., Kim, S., Lebrun, M.H., Bohnert, H., Coughlan, S., Butler, J., Calvo, S., Ma, L.J., Nicol, R., Purcell, S., Nusbaum, C., Galagan, J.E., Birren, B.W., 2005. The genome sequence of the rice blast fungus *Magnaporthe grisea*. Nature 434, 980–986.

Ebbole, D.J., Jin, Y., Thon, M., Pan, H., Bhattarai, E., Thomas, T., Dean, R., 2004. Gene discovery and gene expression in the rice blast fungus, *Magnaporthe grisea*: analysis of expressed sequence tags. Mol. Plant–Microbe Interact. 12, 1337–1347.

Fasters, M.K., Daniels, U., Moerschbacher, B.M., 1993. A simple and reliable method for growing the wheat stem rust fungus, *Puccinia graminis* f. sp. *tritici*, in liquid culture. Physiol. Mol. Plant Pathol. 42, 259–265.

Hahn, M., 2000. The rust fungi. Cytology, physiology and molecular biology of infection. In: Kronstadt, J. (Ed.), Fungal Pathology. Kluwer Academic Publisher, Dordrecht, pp. 267–306.

Hahn, M., Mendgen, K., 1992. Isolation by ConA binding of haustoria from different rust fungi and comparison of their surface qualities. Protoplasma 170, 95–103.

Hahn, M., Mendgen, K., 1997. Characterization of in planta-induced rust genes isolated from a haustorium-specific cDNA library. Mol. Plant–Microbe Interact. 10, 427–437.

Hahn, M., Neef, U., Struck, C., Göttfert, M., Mendgen, K., 1997. A putative amino-acid transporter is specifically expressed in haustoria of the rust fungus *Uromyces fabae*. Mol. Plant–Microbe Interact. 10, 438–445.

Kemen, E., Kemen, A., Rafiqi, M., Hempel, U., Mendgen, K., Hahn, M., Voegele Ralf, R.T., 2005. Characterization of a protein from rust fungi that is transferred from haustoria into the plant host cell. Mol. Plant–Microbe Interact., in press.

Khramtsov, N.V., Woods, K.M., Nesterenko, M.V., Dykstra, C.C., Upton, S.J., 1997. Virus-like, double-stranded RNAs in the parasitic protozoan *Cryptosporidium parvum*. Mol. Microbiol. 26, 289–300.

Lanfranco, L., Novero, M., Bonfante, P., 2005. The mycorrhizal fungus *Gigaspora margarita* possesses a CuZn superoxide dismutase that is up-regulated during symbiosis with legume hosts. Plant Physiol. 137, 1319–1330.

Link, T., Lohaus, G., Heiser, I., Mendgen, K., Hahn, M., Voegele, R.T., 2005. Characterization of a novel $NADP^+$-dependent D-arabitol dehydrogenase from the plant pathogen *Uromyces fabae*. Biochem. J. 389, 289–295.

Liu, Z., Szabo, L.J., Bushnell, W.R., 1993. Molecular cloning and analysis of abundant and stage-specific mRNAs from *Puccinia graminis*. Mol. Plant–Microbe Interact. 6, 84–91.

Mendgen, K., Hahn, M., 2002. Plant infection and the establishment of fungal biotrophy. Trends Plant Sci. 7, 352–356.

Ruepp, A., Zollner, A., Maier, D., Albermann, K., Hani, J., Mokrejs, M., Tetko, I., Guldener, U., Mannhaupt, G., Munsterkotte, M., Mewes, H.W., 2004. The FunCat, a functional annotation scheme for systematic classification of proteins from whole genomes. Nucleic Acids Res. 32, 5539–5545.

Sohn, J., Voegele, R.T., Mendgen, K., Hahn, M., 2000. High level activation of vitamin B1 biosynthesis genes in haustoria of the rust fungus *Uromyces fabae*. Mol. Plant–Microbe Interact. 13, 629–636.

Solomon, P.S., Oliver, R.P., 2002. Evidence that β-aminobutyric acid is a major nitrogen source during *Cladosporium fulvum* infection on tomato. Planta 214, 414–420.

Struck, C., Siebels, C., Rommel, O., Wernitz, M., Hahn, M., 1998. The plasma membrane H^+-ATPase from the biotrophic rust fungus *Uromyces fabae*: Molecular characterization of the gene (*PMA1*) and functional expression of the enzyme in yeast. Mol. Plant–Microbe Interact. 11, 458–465.

Struck, S., Ernst, Hahn, M., 2002. Characterization of a developmentally regulated amino acid transporter (AAT1p) of the rust fungus *Uromyces fabae*. Mol. Plant Pathol. 3, 23–30.

Struck, C., Mueller, E., Martin, H., Lohaus, G., 2004. The *Uromyces fabae* UfAAT3 gene encodes a general amino acid permease that prefers uptake of in planta scarce amino acids. Mol. Plant Pathol. 5, 183–189.

Struck, C., Hahn, M., Mendgen, K., 1996. Plasma membrane H^+-ATPase activity in spores, germ tubes, and haustoria of the rust fungus *Uromyces viciae-fabae*. Fungal Genet. Biol. 20, 30–35.

Thomas, S.W., Rasmussen, S.W., Glaring, M.A., Rouster, J.A., Christiansen, S.K., Oliver, R.P., 2001. Gene identification in the obligate fungal pathogen *Blumeria graminis* by expressed sequence tag analysis. Fungal Genet. Biol. 33, 195–211.

Thara, V.K., Fellers, J.P., Zhou, J.-M., 2003. In planta induced genes of *Puccinia triticina*. Mol. Plant Pathol. 4, 51–56.

Tucker, S.L., Thornton, C.R., Tasker, K., Jacob, C., Giles, G., Egan, M., Talbot, N.J., 2004. A fungal metallothionein is required for pathogenicity of *Magnaporthe grisea*. Plant Cell 16, 1575–1588.

Voegele, R.T., Struck, C., Hahn, M., Mendgen, K., 2001. The role of haustoria in sugar supply during infection of broad bean by the rust fungus *Uromyces fabae*. Proc. Natl. Acad. Sci. USA 98, 8133–8138.

Voegele, R.T., Mendgen, K., 2003. Rust haustoria: nutrient uptake and beyond. New Phytol. 159, 93–100.

Voegele, R.T., Hahn, M., Lohaus, G., Link, T., Heiser, I., Mendgen, K., 2005. Possible roles for mannitol and mannitol dehydrogenase in the biotrophic plant pathogen *Uromyces fabae*. Plant Physiol. 137, 1190–1198.

Wirsel, S.G.R., Voegele, R.T., Bänninger, R., Mendgen, K.W., 2004. Cloning of β-tubulin and succinate dehydrogenase genes from *Uromyces fabae* and establishing selection conditions for their use in transformation. Eur. J. Plant Pathol. 110, 767–777.

Yu, H.J., Lim, D., Lee, H.S., 2003. Characterization of a novel single-stranded RNA mycovirus in *Pleurotus ostreatus*. Virology 314, 9–15.

Zhang, L., Meakin, H., Dickinson, M., 2003. Isolation of genes expressed during compatible interactions between leaf rust (*Puccinia triticina*) and wheat using cDNA-AFLP. Mol. Plant Pathol. 4, 469–477.

Zhang, R., Dickinson, M.J., Pryor, A., 1994. Double-stranded RNAs in the rust fungi. Annu. Rev. Phytopathol. 32, 115–133.